Geometrical Limitations on Attitude Determination for Spinning Spacecraft

James R. Wertz* and Lily C. Chen†
Computer Sciences Corporation, Silver Spring, Md.

Geometrical relationships which limit the determinability of spacecraft attitude parameters are analyzed. Procedures are developed which have reduced the time for prelaunch analysis of attitude observability from a typical several weeks to a few minutes while also providing a broader understanding than previously available. Sun angle, nadir angle, and Sun-to-Earth mid-scan rotation angle measurements are considered for an arbitrary fixed location of the spacecraft; then the effect of orbital motion is considered. The results are summarized in a set of simple geometrical rules. The procedures developed have been used for both prelaunch and postlaunch analysis for various satellites.

Nomenclature

A	= point on celestial sphere in direction of spin axis attitude (Fig. 1)
C	= ratio of attitude component uncertainties defined by Eq. (2)
d	= rotation angle density defined by Eq. (5)
E	= point on celestial sphere in direction of Earth's center (Fig. 1)
m	= attitude measurement
N	= point on celestial sphere in direction of null (S × E)
S	= point on celestial sphere in direction of Sun (Fig. 1)
U_{att}	= largest component of attitude uncertainty
U_m	= component of attitude uncertainty due to measurement m
β	= Sun angle = Sun/attitude angular separation (Fig. 1)
Δm	= change or uncertainty in measurement m
η	= nadir angle = Earth center/attitude angular separation (Fig. 1)
$\Theta_{m/m'}$	= correlation angle = angle of intersection ($\leq 90°$) between attitude loci corresponding to m and m'
Λ	= Sun-Earth-attitude rotation angle (Fig. 1)
ξ	= arc length from null to attitude
Σ	= Earth-Sun-attitude rotation angle (Fig. 1)
Φ	= Sun-attitude-Earth rotation angle (Fig. 1)
ψ	= Sun/Earth center angular separation (Fig. 1)

Superscript

-1	= point on celestial sphere opposite a named point (Fig. 1)

Introduction

THIS paper describes some inherent geometrical restrictions on the accuracy of instantaneous attitude determination for spinning spacecraft. Specifically, relationships between Sun angle, nadir angle, and Sun-to-Earth mid-scan rotation angle measurements are analyzed to identify regions of "poor geometry" in which the attitude uncertainty is large relative to the uncertainty in the measurements. The Sun angle and nadir angle are examples of observables which are essentially the dot product between unit vectors. These are well understood[1-3] and will be treated here only briefly to illustrate the procedures. However, the Sun-Earth rotation angle is a fundamentally different type of measurement; we are unaware of any previous analysis of its geometrical interpretation.

A graphical technique for applying the results obtained to mission planning and prelaunch and postlaunch mission analysis is presented. This technique provides a broad overview of the attitude determination problem and thus permits improved operational results through the use of the best geometrical conditions available within mission constraints. In the year since its development, this technique has been used for attitude accuracy analysis and bias determination planning for the Synchronous Meteorological Satellite-2 (SMS-2), Geostationary Operational Environmental Satellite-1 (GOES-1), Atmospheric Explorer-4 and -5 (AE-4, -5), Communications Technology Satellite (CTS), and the forthcoming Italian satellite, SIRIO.

All of the analysis is carried out on the celestial sphere *centered on the spacecraft* as shown in Fig. 1. Attitude refers to

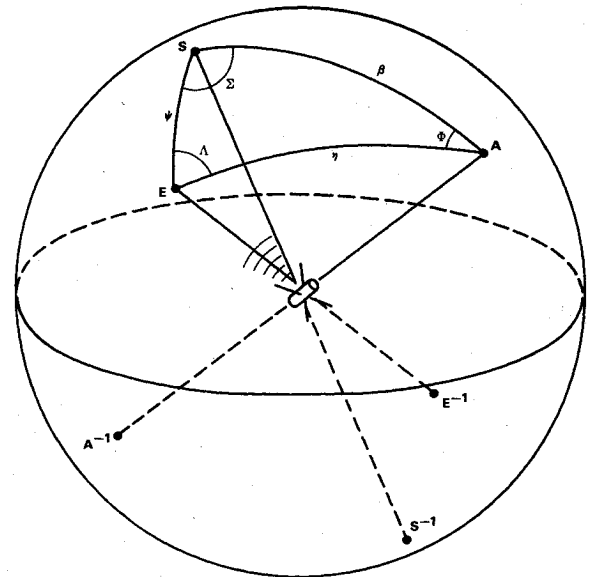

Fig. 1 Definition of angles on a spacecraft-centered celestial sphere (S = Sun, A = attitude, E = Earth).

Presented as Paper AAS75-047 at the AAS/AIAA Astrodynamics Specialist Conference, Nassau, Bahamas, July 28-30, 1975; received Oct. 23, 1975; revision received May 7, 1976. The work was supported by the Attitude Determination and Control Section, Goddard Space Flight Center, NASA under Contract NAS 5-11999. The authors wish to acknowledge the assistance of F.L. Markley.

Index category: Spacecraft Attitude Dynamics and Control.

*Member, Technical Staff, Systems Sciences Division. Member AIAA.

†Member, Technical Staff, System Sciences Division.

the orientation of the spacecraft spin axis. There are two distinct types of measurements involved. The term *arc length* will be used to refer to the angular separation between two directions on the celestial sphere, such as the nadir angle η measured between A and E. In three-dimensional analyses, these are ordinarily referred to as cone angles since they measure the angular radius of a cone. In contrast to arc-length measurements, we will use *rotation angle* for the spherical angle between any two sides of a spherical triangle. Thus, the Sun-attitude-Earth (SAE) rotation angle in Fig. 1 is the spherical angle Φ. Rotation angles are dihedral angles in three-dimensional space, since they measure the angle between two planes. For example, the rotation angle Φ measures the dihedral angle between the attitude vector/Sun vector plane and the attitude vector/nadir vector plane.

In the ordinary process of attitude determination, the location of the Sun and the Earth on the celestial sphere are assumed known.[1,4] A deterministic attitude solution is then obtained from any two of the three measurements β, η, or Φ. The second section of this paper considers the geometry of determining A when S and E are assumed fixed. The third section then describes the effect of allowing the Earth to move across the celestial sphere and presents a graphical technique for analyzing the changing geometry. The basic assumption throughout this paper is that the spacecraft (or at least the sensor) is spinning sufficiently rapidly that the spacecraft orbital motion is completely negligible during the time required for one set of observations of the Earth and Sun.

The analysis presented here can provide information on the correlation of *sensor biases,* parameters which define possible misalignments or miscalibration of attitude sensors. Each of the three measurements has an associated alignment bias which corresponds directly to a change in that measurement. Thus, a misalignment in the elevation of the Sun sensor, called a Sun angle bias, will change the Sun angle measurement by the amount of the misalignment. The bias associated with the rotation angle Φ is called an azimuth bias, and is a relative misalignment in azimuth between the Sun sensor and the Earth sensor. Associated with the nadir angle measurement is an Earth sensor elevation mounting angle bias. For this parameter, the bias and measurement shift will always be in the same direction, but the magnitude of the shift will depend on how far from the center the horizon sensor crosses the disk of the Earth.

Attitude Geometry for a Rapidly Spinning Spacecraft

Geometrical Variables

The attitude, or orientation of the spacecraft spin axis, may be represented as a point on the celestial sphere. Any single attitude measurement, such as the Sun angle, implies that the attitude lies on some curve on the celestial sphere, defined as the loci of all possible orientations of the spin axis corresponding to that particular measurement. If measurement uncertainties imply a range of possible measured values, then the attitude must lie within a band on the celestial sphere. The attitude is determined by intersection of two such bands corresponding to two distinct attitude measurements, such as the Sun angle and the nadir angle.

The uncertainty in the calculated attitude is determined by the size of the region of intersection of the two bands; the size of this region is the subject of this paper. Specifically, the shape of the region of intersection is approximately a parallelogram if it is sufficiently small. The size of the region is determined by two factors – the width of the individual bands and the angle at which they intersect. The width of a band is proportional to the uncertainty in the corresponding measurement and inversely proportional to the density of the constant measurement curves on the celestial sphere. We define the component uncertainty U_m as the width of the band defined by measurement m.

The component uncertainty is trivial to evaluate for Sun angle and nadir angle measurements. A given shift in the Sun angle measurement $\Delta\beta$, corresponds to a shift in the attitude perpendicular to the Sun cone exactly equal to $\Delta\beta$ regardless of the relative positions of the attitude and the Sun. Thus, the density of curves on the celestial sphere for Sun angle measurements is 1. The same is true for nadir angle measurements. Therefore,

$$U_\beta = \Delta\beta \text{ and } U_\eta = \Delta\eta \tag{1}$$

The component uncertainty for rotation angle measurements is more involved because of nonuniformity of the rotation angle curve density. This is discussed in the next section.

It remains to obtain some measure of the attitude uncertainty in terms of the component uncertainties and the angle of intersection of the two bands. Specifically, at any point where two constant measurement curves intersect and have uniquely defined tangent vectors, we will define the *correlation angle* Θ as the rotation angle ($\leq 90°$) between the tangents to the two curves. Then, for an uncertainty region on the celestial sphere sufficiently small for a plane geometry approximation, the maximum attitude uncertainty U_{att} is just the long diagonal of the parallelogram previously defined:

$$U_{att} = \frac{U_m}{\sin\Theta}\sqrt{1+2C\cos\Theta+C^2} \sim \frac{U_m}{\sin[\Theta/(1+C)]}$$

$$C = U_{m'}/U_m \leq 1 \tag{2}$$

where U_m is the component uncertainty caused by the more uncertain of the two measurements, and $U_{m'}$ is the component uncertainty of the remaining measurement. The approximate form on the right-hand side of Eq. (2) is valid for either small values of Θ or for C close to 1. Note that the range of the quantity in square brackets is $\Theta/2$ to Θ. Throughout this paper, *attitude uncertainty* will refer to the largest component of the uncertainty region. A region of *bad geometry* will be defined as any region in which the largest component of the attitude uncertainty determined from the intersection of two measurements is more than 5 times greater than the measurement uncertainty, assuming equal uncertainties in the two measurements. The factor 5 is arbitrarily chosen for illustration and approximates the relevant value for several recent missions.[6] From Eq. (2), with $C=1$, it is seen that for unit curve density this corresponds to a region in which the correlation angle is less than 23.1°. In equations for finding specific values of Θ [Eqs. (4, 6, and 7)], it is convenient to let Θ cover the full range of $0 \leq \Theta \leq 360°$. When a value for Θ lies outside the range $0 \leq \Theta \leq 90°$, the following change of "phase" in Θ should be carried out:

$$\Theta \rightarrow 360° - \Theta \quad \text{if } 270° \leq \Theta \leq 360° \tag{3a}$$

$$\Theta \rightarrow |180° - \Theta| \quad \text{if } 90° < \Theta < 270° \tag{3b}$$

The correlation angle takes on a particularly simple form for β/η correlations. A given value of β or η implies that the spacecraft attitude lies on a small circle on the celestial sphere centered on the Sun or the Earth with a radius equal to the measured arc length. The angle between the tangents to the two small circles at their intersection is equal to the angle between the two radii at that point. But this is just the Sun-attitude-Earth rotation angle Φ. Thus,

$$\Theta_{\beta/\eta} = \Phi \tag{4}$$

where the phase restrictions of Eq. (3) hold. $\Theta_{\beta/\eta}$ will be 0 when the Sun, Earth, and attitude are coplanar. When this occurs, β and η provide the same information, so no information is available on the attitude component perpendicular to the Earth-Sun great circle. In addition, biases in

the two correlated measurements have the same effect on the data and are effectively indistinguishable. Thus, along the Earth-Sun great circle, a Sun angle bias will be indistinguishable from an Earth sensor elevation mounting angle bias.

Rotation Angle Measurements

A fixed SAE rotation angle Φ implies that the spin axis attitude of the spacecraft is constrained to lie on a curve with two discrete segments on the celestial sphere. Representative plots of these constant Φ curves are shown in Figs. 2-4 for Earth-Sun arc-length separations of 30° and 90°. The underlying coordinate grid for the plots is a celestial globe with geometry as viewed from infinity, i.e., in these *orthographic projections* half of the globe is seen in each view. The grid has 10° intervals in latitude and longitude, except within 10° of the poles. The equator on all plots is a slightly heavier line for ease of identification. The spacecraft is assumed to be at the center of the sphere and the Sun (S) is at the North Pole. The locations of the Earth (E) and the zenith (E^{-1}) are indicated by arrows. A third important reference direction is the null (N) or Sun vector/nadir vector cross product, which lies on the equator 90° in azimuth from the Sun-Earth great circle.

The curves overlying the coordinate grid are lines of Φ = constant. For example, the curve labeled "40°" covers all possible orientations of the spacecraft spin axis such that the rotation angle from the Sun to the Earth (about the attitude axis) is 40°. Thus, the set of constant Φ curves has the same relation to the SAE rotation angle measurement as the set of all small circles centered on the Sun has to the Sun angle measurement.

Figures 2 and 3 show five views of the rotaion angle geometry for an angular separation of the Sun and the Earth of 30°. The views are centered at varying Sun angles β and azimuth angles relative to the Earth-Sun line (called "Azimuth" in the captions). The rotation angle curves are plotted in 10° intervals, except in Fig. 3c, in which 25° and 35° curves have been added as dotted lines to show the shape of curves in the region of the null. Curves between 120 and 240° (or above 90° in Fig. 3c) have been omitted because of the high density.

The general character of the rotation angle curves is evident from the plots. As can be seen most clearly in Figs. 3a and 3d, the great circle containing the Earth and the Sun divides the celestial sphere into two hemispheres. All rotation angle curves between 0° and 180° are in one hemisphere and all curves between 180° and 360° are in the other. In addition, the 30 and 330° rotation angle curves (i.e., the curves with $\Phi = \psi$) divide each hemisphere into four quadrants, as can be seen in Fig. 3c. Also from Fig. 3c it can be seen that each rotation angle curve (except those of 30° and 330°) consists of two nonintersecting segments in opposite quadrants of one hemisphere. All segments start and end on the Earth, Sun, zenith, or antisolar point.

In contrast to the uniformly distributed small circles of β and η, the rotation angle curves are characterized by their greatly varying density. For $\psi < 90°$, the rotation angle density is greatest between the Earth and the Sun (and between the zenith and the anti-solar point) and least in the region of the null or the anti-null. A low rotation angle density means

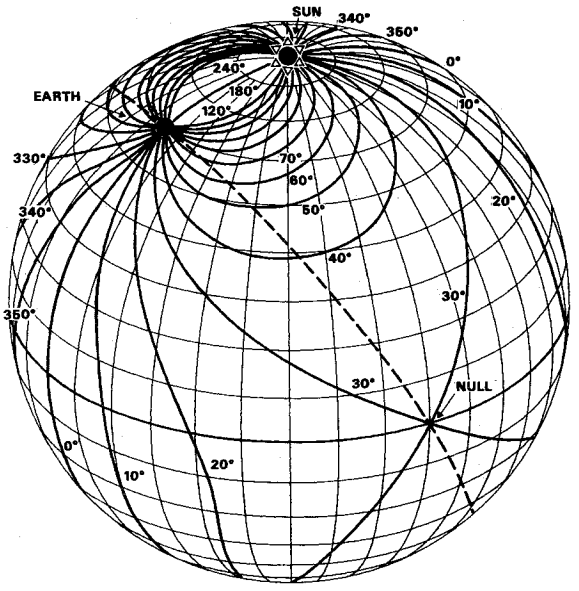

Fig. 2 Rotation angle geometry for a 30° Sun-Earth angular separation. View centered at $\beta = 60°$, azimuth = 60°.

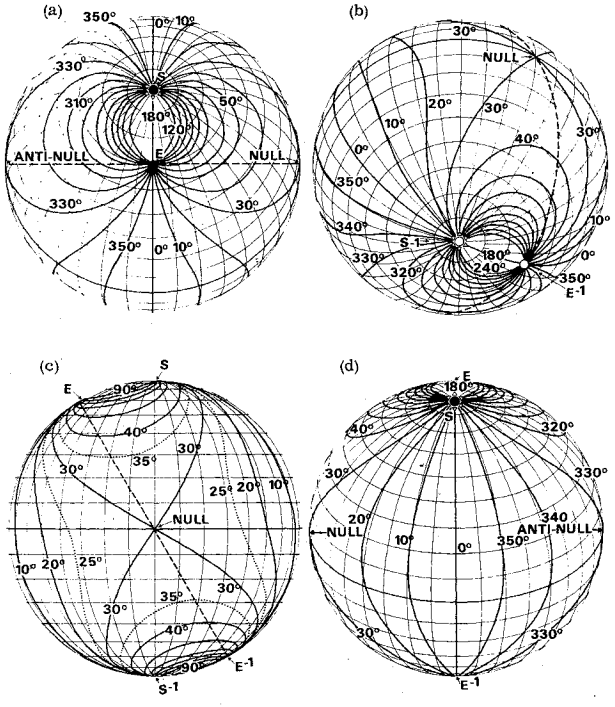

Fig. 3 Different views of rotation angle geometry for a 30° Sun-Earth angular separation. Views centered at (β, azimith) coordinates of: a) 30°, 0°); b) 150°, 60°); c) (90°, 90°); and d) 60°, 180°).

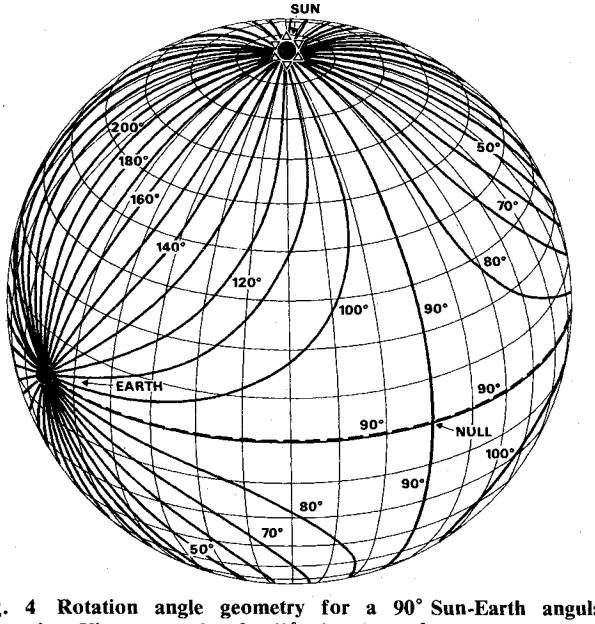

Fig. 4 Rotation angle geometry for a 90° Sun-Earth angular separation. View centered at $\beta = 60°$, azimuth = 60°.

that a small change in the rotation angle corresponds to a large change in the attitude. From Fig. 3c, it can be seen that a change of only 5° in rotation angle near the null (from 30° at the null to either 25° or 35°) corresponds to a shift in attitude from the null to a point over 30 arc-degrees away. Thus, the region around the null or the anti-null will be an area of poor rotation angle attitude solutions, since a small uncertainty in rotation angle corresponds to a large uncertainty in attitude. Similarly, for the geometry of Fig. 3, the area between the Earth and the Sun (or between the zenith and the anti-solar point) will result in particularly good rotation angle attitude solutions.

The extent of the region of poor attitude solutions in the vicinity of the null may be explicitly determined for any given Sun-Earth arc-length separation ψ by evaluating the rotation angle density d. Specifically, as the attitude approaches the null or anti-null from the direction of the midpoint on the celestial sphere between the Earth and the Sun or between the zenith and the anti-solar point, the rotation angle density is given by

$$d = \frac{\partial \Phi}{\partial \xi}\bigg|_{\perp} = \frac{\sin\psi \sin\xi}{1-\cos^2(\psi/2)\sin^2\xi} \tag{5}$$

where ξ is the arc-length distance from the null to the attitude. (As the attitude approaches the null or anti-null from the perpendicular direction, the same equation holds with ψ replaced by $90° - \psi$.) A derivation of Eq. (5) is given in Appendix A. Equation (5) implies a vanishing rotation angle density at the null and a finite-limiting density at the point midway between the Earth and the Sun (or the zenith and the anti-solar point).

Figure 4 shows the rotation angle curves for an Earth-Sun separation of 90°. Thus, the Earth moves down to the equator of the underlying coordinate grid, and the Sun, Earth, and null form an equilateral right spherical triangle. The regions between the Earth and the Sun and between the Earth and the anti-solar point become equivalent in terms of rotation angle density. In general, the rotation angle curves have become more uniformly distributed over the celestial sphere, although a large region of low density remains in the vicinity of the null and the anti-null. The 90° and 270° rotation angle curves that form the boundaries of the four quadrants in each hemisphere are great circles with the one connecting the Earth and the zenith lying along the equator of the coordinate grid. When $\psi > 90°$, the geometry is equivalent to that of $\psi < 90°$ with the location of the Earth and the zenith interchanged.

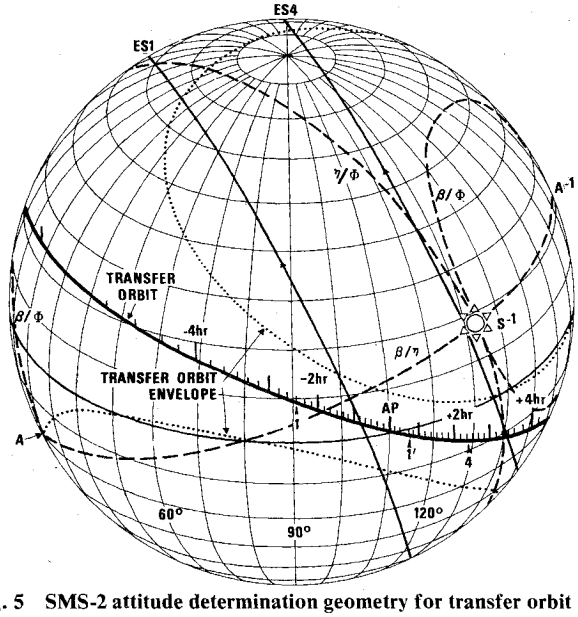

Fig. 5 SMS-2 attitude determination geometry for transfer orbit and apogee motor firing attitude.

In general, rotation angle geometry is more complex than arc-length geometry. It is also more restrictive in that large regions of the celestial sphere exist where low rotation angle densities imply poor attitude solutions without regard to the nature of the arc-length curves that are used in conjunction wth the rotation angle curves.

Intersection of Arc-Length and Rotation Angle Measurements

Two of the three fundamental procedures for determining attitude involve the intersection of an arc-length measurement and a rotation angle measurement. That is, the SAE rotation angle Φ may be combined with either the Sun angle β or the nadir angle η to determine the attitude. Most of the discussion here is limited to β/Φ intersections. However, all of the results apply equally to η/Φ intersections, as is clear from the symmetry of the rotation angle curves with respect to interchanging the Sun and the Earth. Figures 2-4 are convenient for studying the general character of β/Φ intersections because a fixed β implies that the spacecraft attitude lies on a small circle centered on the Sun. Therefore, the latitude lines on the underlying coordinate grid are constant β curves.

The concept of correlation angle can be applied to the case of the intersection of an arc-length measurement and a rotation angle measurement. Thus, in Figs. 2-4, the β/Φ correlation angle $\Theta_{\beta/\Phi}$ is simply the angle between the constant rotation angle curves and the constant β curves. As shown in Appendix B

$$\Theta_{\beta/\Phi} = \arctan\left[\frac{\tan\eta}{\tan\beta \sin\Phi} - \cot\Phi\right] \tag{6}$$

with the phase restrictions of Eq. (3).

As is most easily seen in Fig. 2 and 3c, the only condition under which $\Theta_{\beta/\Phi} = 0$ is when the attitude lies on the great circle containing the Earth, zenith, null, and anti-null, shown as a dashed line on the plots. When the attitude lies on the Earth-null great circle, β and Φ are providing the same information and no information is available on the component of the attitude along the constant β and Φ curves. Along the Earth-null

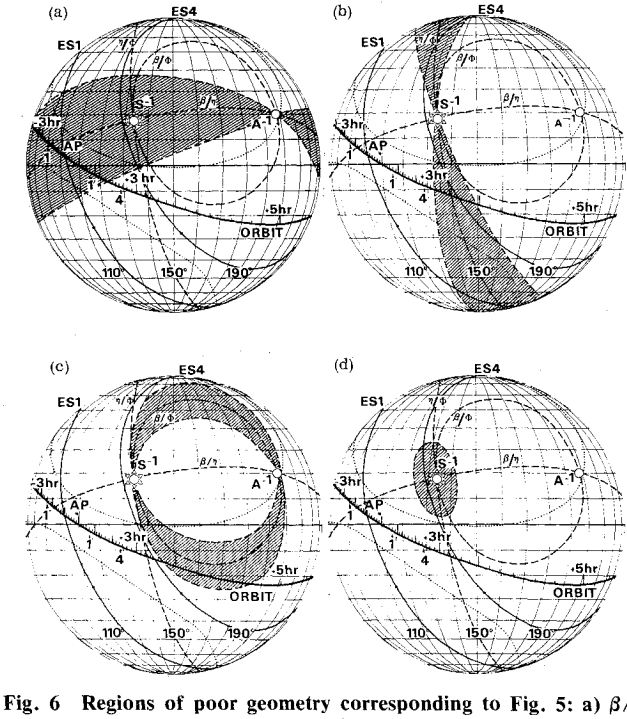

Fig. 6 Regions of poor geometry corresponding to Fig. 5: a) β/η correlation; b) η/Φ correlation; c) β/Φ correlation; d) low rotation angle density.

great circle, a Sun angle bias will be indistinguishable from an Earth sensor azimuth bias.

By symmetry with Eq. (6), we may immediately obtain the expression for the η/Φ correlation angle as

$$\Theta_{\eta/\Phi} = \arctan\left[\frac{\tan\beta}{\tan\eta\sin\Phi} - \cot\Phi\right] \tag{7}$$

again with the phase restrictions of Eq. (3). $\Theta_{\eta/\Phi}=0$ when the attitude lies on the Sun-null great circle. Along this great circle, η and Φ will be correlated and an Earth sensor elevation mounting angle bias will be indistinguishable from an Earth sensor azimuth bias.

Effect of Spacecraft Orbital Motion

As the spacecraft moves in its orbit, the attitude determination geometry changes due to the motion of the position of the Earth (as seen by the spacecraft) relative to the Sun and the attitude. A convenient vehicle for examining this geometry as the Earth moves is a plot of the celestial sphere as seen by the spacecraft with the directions of the Sun and the attitude fixed. Figures 5 and 6 show examples of such plots for the nominal transfer orbit and apogee motor firing attitude of SMS-2 launched on February 6, 1975. Plots similar to those of Figs. 5 and 6 contain essentially all of the necessary information on attitude determination geometry and are in regular use by the authors for prelaunch and postlaunch analysis for various spacecraft. For convenience, the plots are now computer generated and plotted on a CalComp plotter. However, it takes only a few minutes to construct one by hand on a printed coordinate grid identical to the one used for the background in all of the figures in this paper.

The underlying coordinate grid in Figs. 5 and 6 is the celestial coordinate system with lines at 10°intervals in both right ascension and declination. Fig. 5 is centered at 90°right ascension and +30°declination. Fig. 6 is centered at 150°right ascension and 0°declination. In all of the plots, the spacecraft is assumed to be at the center of the sphere. The heavy solid line is the orbit of the Earth around the spacecraft as seen from the spacecraft. The Earth is moving toward increasing right ascension, i.e., from left to right on the plots. Tick marks are times from apogee in 10-min intervals. The dotted line surrounding the orbit marks the envelope of the disk of the Earth as it moves across the sky. AP marks the location of apogee. S^{-1}, A, and A^{-1} mark the location of the anti-solar point, attitude, and negative attitude axis, respectively.

The small circles labeled ES1 and ES4 and centered on the $A\text{-}A^{-1}$ axis (approximately straight lines going from lower right to upper left on Fig. 5) are the field of view (FOV) lines of two of the five SMS-2 Earth horizon sensors as the spacecraft spins about the $A\text{-}A^{-1}$ axis. Arrowheads on the FOV lines indicate the direction in which the sensors scan the sky. Acquisition (AOS) and loss (LOS) of the Earth by each sensor are indicated by arrowheads with primed numbers (LOS) or unprimed numbers (AOS) along the orbit.

The three dashed curves on the plots are the center lines of regions of poor geometry for attitude and bias determination caused by a strong correlation among attitude determination procedures or, equivalently, among biases. One of the three correlation angles, $\Theta_{\beta/\eta}$, $\Theta_{\beta/\Phi}$, or $\Theta_{\eta/\Phi}$, is zero along each of the dashed curves indicated in Fig. 5 by "β/η,", "β/Φ," and "η/Φ," respectively. Note that the bad geometry regions in Figs. 5 and 6 are the locations of the Earth for which the correlation geometry *evaluated at the attitude*, will give poor attitude determination results. To evaluate this geometry directly, it is necessary to reformulate Eqs. (4, 6, and 7) so that ths position of the Earth becomes the dependent variable. The poor geometry regions may then be added to the celestial sphere plot, and the position of the Earth during periods of coverage by various sensors may then be evaluated in terms of the attitude and bias determination geometry. Figure 6 shows the individual bad geometry regions as shaded areas. The viewing orientation of the spheres in Fig. 6 is shifted down and to the right from Fig. 5 in order to show the full extent of the poor geometry regions.

For the β/η correlation, Eq. (4) may be used directly. Since $\Theta_{\beta/\eta}=\Phi$, the poor geometry region will lie between two great circles which intersect at A and A^{-1} and which are at an angle $\Theta_{\beta/\eta}$ on either side of the Sun-attitude great circle. The extent of the region for $\Theta_{\beta/\eta}=23.1°$ is shown by the shaded area in Fig. 6a. Clearly, the fractional area of the celestial sphere covered by this region is $\Theta_{\beta/\eta}/90°$.

For the η/Φ correlation, Eq. (7) may be reformulated as

$$\cot\Sigma = \tan\Theta_{\eta/\Phi}\cos\beta \tag{8}$$

where Σ is the attitude-Sun-Earth rotation angle defined in Fig. 1. This implies that when $\Theta_{\eta/\Phi}=0°$, $\Sigma=90°$ and, therefore, the Earth must lie on the great circle through the sun perpendicular to the Sun-attitude great circle marked η/Φ on Fig. 5. This is equivalent to the attitude lying on the great circle containing the Sun and the null, as discussed earlier. The poor geometry region around the η/Φ great circle will be bounded by two great circles intersecting at the Sun and making an angle of magnitude $|90°-\Sigma|$ with the η/Φ great circle, where Σ is given by Eq. (8). The shaded area in Fig. 6b shows this region for $\Theta_{\eta/\Phi}=23.1°$ and the Sun angle from Fig. 5($\beta\sim60°$). This region is smaller in area than the β/η poor geometry region, except in the limit of $\beta=0°$ or 180° when the two regions are of equal area.

By symmetry with Eq. (8), Eq. (6) for the β/Φ correlation may be rewritten as

$$\cot\Lambda = \tan\Theta_{\beta/\Phi}\cos\eta \tag{9}$$

Note that this equation must be solved numerically, since the right-hand side is not independent of the position of the Earth for nonzero correlation angles. However, when $\Theta_{\beta/\Phi}=0°$, Λ must be a right angle. When $\Lambda=90°$, the attitude lies on the Earth-null great circle, as required by earlier results, and the central line of the β/Φ bad geometry region is the 90° or 270° constant rotation angle curve between the Sun and the attitude. This is the curve labeled β/Φ in Figs. 5 and 6. The shape of the poor geometry region for the geometry of Fig. 5 and a correlation angle of 23.1° is shown by the shaded area

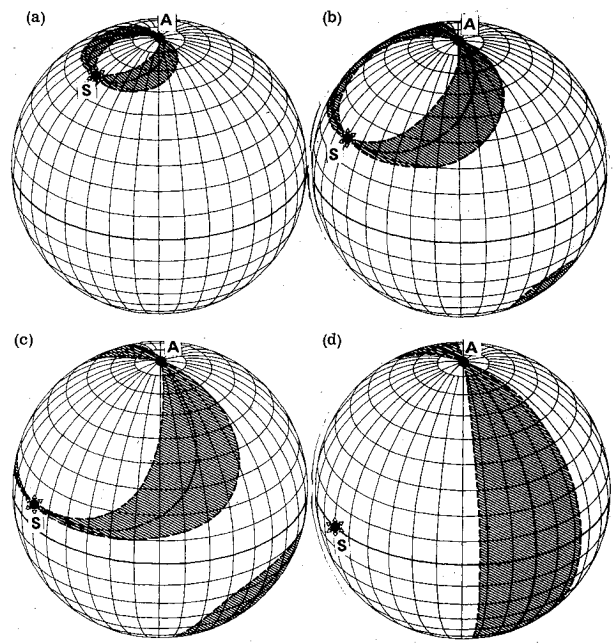

Fig. 7 Evolutions of β/Φ correlation poor geometry region for Sun-attitude separations of 30°, 60°, 80°, and 90°.

in Fig. 6c. Figure 7 shows the evolution of the shape of this region for $\Theta_{\beta/\Phi}=23.1°$ and values of the Sun-attitude separation of 30°, 60°, 80°, and 90°. As seen most clearly in Fig. 7c, this region is *not* symmetric under an interchange of S and A. Except for a Sun angle of 90°, the β/Φ correlation region consists of two unconnected areas, one near A and the other near A^{-1}.

Finally, in addition to the poor geometry regions caused by measurement and bias correlations, the shaded area in Fig. 6d shows the poor geometry region due to the low rotation angle density discussed earlier. If the Earth lies inside the shaded region (or an identical region about the Sun), the rotation angle density, evaluated at the attitude, will be less than 0.2. Thus, these are the *locations of the Earth* for which there is poor attitude determination geometry due to a low rotation angle density *at the attitude.* Figure 8 shows the evolution of the shape of the region for Sun-attitude separations of 30°, 60°, 80°, and 90°. The outer, middle, and inner curves in each plot are for rotation angle densities of 0.5, 0.2, and 0.1, respectively. Each of the global projection plots in Fig. 8 is centered on the Sun.

The angular radius of the low rotation angle density region along the η/Φ correlation great circle ($\Sigma=90°$) and the Sun-attitude great circle ($\Sigma=0°$ or 180°) is given by

$$\psi_0=\beta-\text{arc cot}\,(\cot\beta+d) \quad (\Sigma=0°;\ \eta\leq\beta) \tag{10a}$$

$$\psi_{180}=-\beta+\text{arc cot}\,(\cot\beta-d) \quad (\Sigma=180°;\ \eta\geq\beta) \tag{10b}$$

$$\psi_{90}=\text{arc tan}\left(\frac{\cot^2\beta}{d^2}-1\right)^{-1/2}\sin\beta \quad (\Sigma=90°,\ 270°) \tag{10c}$$

where $d=\partial\Phi/\partial\xi$ is the rotation angle density.

Summary of Analytic Results

The correlation angle Θ, for any pairwise combination of the three basic attitude measurements considered (Sun angle, nadir angle, and SAE rotation angle), may be evaluated for any relative position of the Sun, Earth, and attitude by use of Eqs. (4,8, and 9). Θ may then be used to determine the attitude uncertainty in terms of the measurement uncertainties via Eq. (2). These equations may also be used to identify areas of unfavorable geometry on the celestial sphere. Specifically, for a given position of the Sun and the attitude, the following locations of the Earth are regions of poor geometry for spacecraft attitude and bias determination:

1) The Sun angle/nadir angle correlation region (β/η) is centered on the Sun-attitude great circle. For a given correlation angle, the boundaries of the poor geometry region are great circles given by Eq. (4), as shown in Fig. 6a. This region has the largest area of the three correlation regions. Within the β/η correlation region, Sun angle/nadir angle attitude solutions have large uncertainties and the Sun angle bias and Earth sensor elevation mounting angle bias are nearly indistinguishable.

2) The nadir angle/SAE rotation angle correlation region (η/Θ) is centered on the great circle through the Sun perpendicular to the Sun-attitude great circle. The boundaries of the poor geometry region are great circles given by Eq. (8), as shown in Fig. 6b. The area of the region depends on the Sun angle and is largest for a Sun angle of 0° or 180°, where it is equal to the β/η correlation area. Within this region, the nadir angle/SAE rotation angle attitude solutions have large uncertainties and the Earth sensor elevation mounting angle bias and Earth sensor azimuth bias are nearly indistinguishable.

3) The two Sun angle/SAE rotation angle correlation regions (β/Φ) are centered on the curves which maintain a constant 90° or 270° rotation angle from the Sun to the attitude (SAE rotation angle). The boundaries of the poor geometry region are given by Eq. (9) and are shown in Fig. 6c. The shape of the region for representative Sun angles is shown in Fig. 7. The area of the region depends on the Sun angle and is largest for a Sun angle of 90° where it is equal to the β/η correlation area. Within the β/Φ correlation region the Sun angle/SAE rotation angle attitude solutions have uncertainties and the Sun angle bias and Earth sensor azimuth bias are nearly indistinguishable.

4) The two regions of low rotation angle density are approximately elliptical areas around the Sun and anti-solar point and extend along the great circle from the Sun perpendicular to the Sun-attitude great circle as shown in Fig. 6d. Equations for the distance from the Sun to the boundary of the region along several great circles are given by Eqs. (10). The shape of the region for representative Sun angles is shown in Fig. 8. When the Earth lies within this region, attitude solutions based on the SAE rotation angle will have large uncertainties.

These regions may be compared with the position of the Earth during coverage by various sensors to judge the determinability of spacecraft attitude and bias parameters.

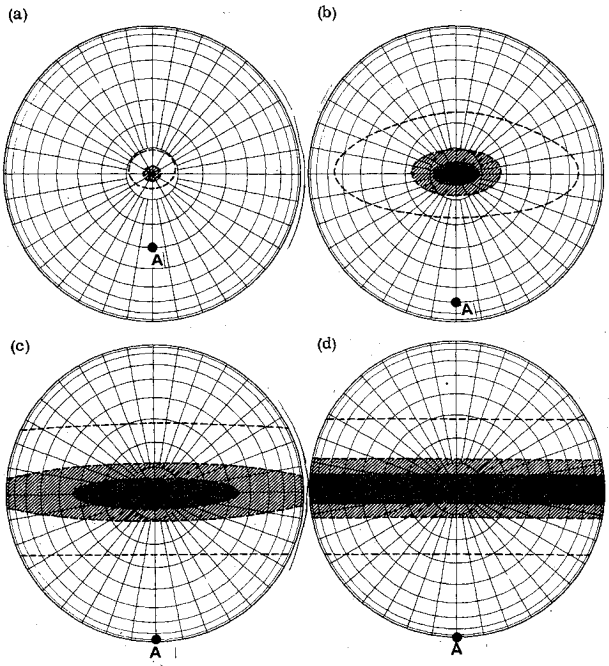

Fig. 8 Evolution of poor geometry region due to low rotation angle density for Sun-attitude separation of 30°, 60°, and 90°. Sun is atcenter of each figure. When Earth lies inside shaded region, rotation angle density, evaluated at attitude, will be less than 0.2.

Interpretation of Geometry Plots

We will illustrate the practical application of these geometry plots by analyzing the example shown in Figs. 5 and 6 of the SMS-2 spacecraft in a transfer orbit to synchronous altitude. Figure 5 shows the geometry before and at apogee and Fig. 6 shows the geometry after apogee. The region around perigee is of little interest in this case, since the spacecraft is out of contact with the Earth at perigee.

Earth sensor 1, ES1, was designated as the prime attitude sensor. As seen from Fig. 5, this sensor picks up the Earth 2½ hr before apogee and ½ hr before the Earth crosses the $\Theta_{\beta/\eta}=0°$ great circle. As seen from Fig. 6a, the entire coverage of ES1 is within the β/η poor geometry region. This implies that the Sun angle/nadir angle solutions will have large uncertainties and that a Sun angle bias cannot be distinguished from an Earth sensor elevation mounting angle bias with data from ES1. However, if the Sun angle bias is determined using other sensor data and held fixed during the processing of ES1 data, then this data can be used to determine the ES1 elevation mounting angle bias and azimuth bias.

It should be possible to determine a Sun angle bias with data from ES4 after apogee. The η/Φ and β/Φ correlation regions occur near the beginning of data from ES4. Simulation results indicate that although there is a strong correlation, the Sun angle bias can be resolved with sufficient data near perigee.[5,6] The procedure of using ES4 data to determine the Sun angle bias and ES1 data to determine the other ES1 biases was adopted and used successfully for mission support.[5-7] Similar procedures were used for other phases of the mission. Data collected primarily on the basis of analysis of the geometry plots was used to determine 20 attitude bias parameters for five Earth sensors and one Sun sensor.

Discussion

Each of the prelaunch conclusions relative to SMS-2 attitude and bias observability was confirmed with both real and simulated data using both a deterministic processor and a recursive least-squares bias determination filter.[5-8] Similar results have been obtained on four subsequent missions (GOES-1, AE-4, AE-5, and CTS), although none have had as extensive a bias determination sequence as SMS-2.

The geometrical system presented here provides either quick qualitative division of the celestial sphere into regions of "good and "bad" geometry for attitude and bias determination, or a numerical algorithm to evaluate the attitude uncertainty in terms of the measurement uncertainties for any point on the celestial sphere. The principal limitation of the system is that it does not provide for integration of the effects of variation of the geometry over large data spans, such as a full orbit. A system for carrying out the integration of geometrical effects has been proposed.[9]

The geometrical procedures of this paper are applicable to nearly all phases of mission attitude planning and analysis. Although numerous simulation runs were made for SMS-2 to verify the conclusions reached from the geometry plots, the prelaunch analysis of attitude and bias determinability was several times more extensive for SMS-2 than it had been for SMS-1 when this geometrical analysis was not available. During the course of the SMS-2 prelaunch analysis, it was straightforward to find new sensor orientations which would test particular aspects of the geometry. This implies that the geometrical analysis may be of use in mission planning to determine the most effective orientation for horizon sensors or the best choice of sensor mounting angle for panoramic Earth sensors, such as those used on Radio Astronomy Explorer satellites.[10] Using the procedures presented here, analysis is now in progress of Sun-to-Earth horizon rotation angles, a measurement which is neither a pure rotation angle nor an arc length.

Appendix A

Figure A-1a shows the geometry on the celestial sphere when the attitude is located on the great circle passing through the null and midway between S and E. By definition of the null, arc lengths NE, NB, and NS are 90°, as are rotation angles NBE and NBS. By symmetry and simple spherical geometry

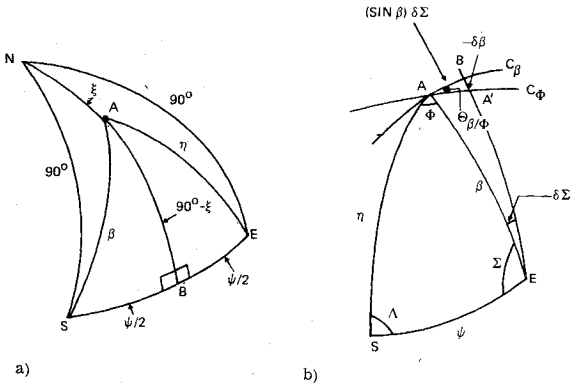

Fig. A-1 Definition of geometrical variables.

$$\beta = \eta \tag{A1}$$

$$\cos\eta = \cos(\psi/2)\cos(90° - \xi) \tag{A2}$$

$$\cos\psi = \cos\eta\cos\beta + \sin\eta\sin\beta\cos\Phi \tag{A3}$$

Substituting Eqs. (A-1) and (A-2) into Eq. (A-3) yields

$$\cos\Phi = (\cos\psi - a)/(1-a) \tag{A4}$$

where $a = \cos^2(\psi/2)\sin^2\xi$. To obtain the rotation angle density d, we differentiate Eq. (A4) with respect to ξ, which gives

$$(\sin\Phi)\frac{\partial\Phi}{\partial\xi} = \frac{\sin^2\psi\sin\xi\cos\xi}{(1-a)^2} \tag{A5}$$

But from Eq. (A4):

$$\sin\Phi = [1-\cos^2\Phi]^{1/2} = \frac{\sin\psi\cos\xi}{1-a} \tag{A6}$$

Therefore, substituting Eq. (A6) into Eq. (A5), we obtain

$$d = \frac{\partial\Phi}{\partial\xi} = \frac{\sin\psi\sin\xi}{1-a} = \frac{\sin\psi\sin\xi}{1-\cos^2(\psi/2)\sin^2\xi} \tag{A7}$$

Appendix B

The geometry for deriving the correlation angle $\Theta_{\beta/\Phi}$ is given in Fig. A-1b. C_Φ and C_β are the constant Φ and constant β curves through A. By definition, $\Theta_{\beta/\Phi}$ is the angle between C_β and C_Φ. Let the attitude move an infinitesimal amount from A to A′ along C_Φ; then β will change by $-\delta\beta$ perpendicular to C_β, and Σ will change by $\delta\Sigma$ which gives an arc-length change along C_β of $\delta\Sigma\sin\beta$ (arc AB). From the infinitesimal right triangle ABA′, we obtain

$$\tan\Theta_{\beta/\Phi} = \frac{-\delta\beta}{\sin\beta\delta\Sigma}\bigg|_\Phi = -\frac{1}{\sin\beta}\frac{\delta\beta}{\delta\Sigma}\bigg|_\Phi \tag{B1}$$

From the spherical triangle AES, we have

$$\cot\psi\sin\beta = \cos\beta\cos\Sigma + \cot\Phi\sin\Sigma \tag{B2}$$

$$\cot\eta\sin\beta = \cos\beta\cos\Phi + \cot\Sigma\sin\Phi \tag{B3}$$

By differentiating Eq. (B2), we obtain

$$\frac{\delta\beta}{\delta\Sigma}\bigg|_\Phi = \frac{\cot\Phi\cos\Sigma - \cos\beta\sin\Sigma}{\cot\psi\cos\beta + \sin\beta\cos\Sigma} \tag{B4}$$

Substituting Eq. (B2) into Eq. (B4) to eliminate cot ψ gives

$$\frac{\delta\beta}{\delta\Sigma}\bigg|_\Phi = \sin\beta\frac{\cot\Phi\cot\Sigma - \cos\beta}{\cot\Sigma + \cot\Phi\cos\beta} \tag{B5}$$

Then, eliminating cot Σ by substituting Eq. (B3) into Eq. (B5), we get

$$\frac{\delta\beta}{\delta\Sigma}\bigg|_\Phi = \frac{1}{\sin\Phi}[\cos\Phi\sin\beta - \tan\eta\cos\beta] \tag{B6}$$

Finally, substituting Eq. (B6) into Eq. (B1), we obtain

$$\Theta_{\eta/\Phi} = \arctan\left[\frac{\tan\eta}{\tan\beta\sin\Phi} - \cot\Phi\right] \tag{B7}$$

References

[1]Werking, R.D., ed., "A Generalized Technique for Using Cones and Dihedral Angles in Attitude Determination," NASA, X-542-71-222, June 1971.

[2]Shear, M.A., "Optical Aspect Attitude Determination System (OASYS) Version 4.0 System Description and Operating Guide," Computer Sciences Corp., Silver Spring, Md., 3000-0600-03TM, Dec. 1973.

[3]Hanson, C.W. and Brown, J.V., "Attitude Determination for the SKYNET and NATO Synchronous Communications Satellites," *AIAA Progress in Astronautics and Aeronautics: Communication Satellite Technology*, Vol. 33, edited by P.L. Bargellini, MIT Press, Cambridge, Mass., 1974, pp. 127-140.

[4]Albus, J.S., Muckel, G.A., and Pyle, E.J., "Attitude Determination of a Spin Stabilized Spacecraft," NASA, X-711-68-336, Aug. 1968.

[5]Chen, L.C. and Wertz, J.R., "Analysis of SMS-2 Attitude Sensor Behavior Including OABIAS Results," Computer Sciences Corp., Silver Spring, Md., CSC/TM-75/6003, April 1975.

[6]Chen, L.C., Chou, C., and Wertz, J.R., "SMS-B Attitude and Bias Determination Geometry," Computer Sciences Corp., Silver Spring, Md., 3000-29100-06TN, Jan. 1975.

[7]"SMS-2 Flight Dynamics Postlaunch Report," in preparation, NASA.

[8]Wertz, J.R. and Chen, L.C., "Geometrical Procedures for the Analysis of Spacecraft Attitude and Bias Determinability," Paper AAS75-047, Nassau, Bahamas, 1975.

[9]Wertz, J.R., Chen, L.C., and Liu, K.S., "Bias and Attitude Determinability Prediction System (BAD) Analytic Basis," Computer Sciences Corp., Silver Spring, Md., CSC/TM-75/6007, in press.

[10]Werking, R.D., "Radio Astronomy Explorer-B Postlaunch Attitude Operations Analysis," NASA, X-581-74-227, July 1974.